Large-Signal Transient Analysis of Forward Converter with Active-Clamp Reset

Qiong Li and Fred C. Lee
Virginia Power Electronics Center
The Bradley Dept. of Electrical Engineering
Virginia Polytechnic Institute and State University
Blacksburg, VA 24061
USA

Milan M. Jovanović
Delta Power Electronics Lab., Inc.
1872 Pratt Drive, Suite 1400
Blacksburg, VA 24060
USA

Abstract -- The forward converter with the active-clamp reset offers many advantages over the forward converter with other transformer reset methods. However, during the line and load transients, the maximum magnetizing current of the transformer and the peak voltage of the primary switch are strongly affected by the active-clamp circuit dynamics. As a result, the design of a forward converter with the active-clamp reset cannot be optimized based only on its dc characteristics. In this paper, a large-signal analysis of the forward converter with the active-clamp reset and output-voltage feedback control is presented. The analysis can be used to predict converter's dynamic performance.

I. INTRODUCTION

The forward converter is one of the most popular switching topologies for low and medium power applications. To achieve high efficiency at higher switching frequencies, an active-clamp reset circuit is often applied across the main switch [1]. The function of the active-clamp reset circuit is to provide the flux reset of the core of the power transformer, thus eliminating the need for additional winding or a dissipative RCD-clamp reset. A number of papers have discussed many design issues which relate to the active-clamp reset mechanism [2-6], but no explicit analysis has been presented so far for the large signal transient response. Since during large-signal transients, the active-clamp-circuit dynamics strongly affects the maximum magnetizing current of the transformer and the peak voltage of the primary switch, the design of a forward converter with the active-clamp reset cannot be optimized based only on its dc characteristics.

In this paper, an average state trajectory approach is used to analyze the response of the active-clamp circuit with output-voltage feedback control during line and load transients. It is shown that in addition to the selection of transformer parameters and the active-clamp capacitance, the control loop bandwidth is a design parameter which determines the maximum voltage of the main power switch and magnetizing current of the transformer during transients.

II. LARGE-SIGNAL TRANSIENT BEHAVIOR

The forward converter power-stage with the active-clamp reset is shown in Fig. 1. The active-clamp reset circuit consists of the series connection of auxiliary switch S_2 and clamp capacitor C_C. It should be noted that transformer in Fig. 1 is shown as a parallel connection of the magnetizing inductance L_M and the ideal transformer with a turns-ratio $n=\frac{N_P}{N_S}$.

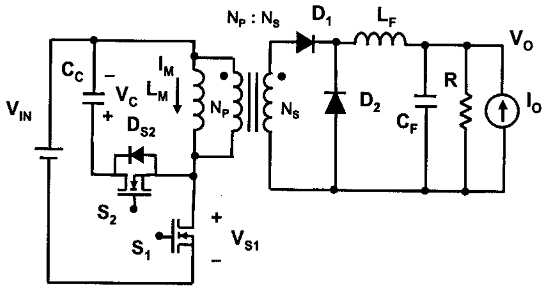

Fig. 1. Active-clamp forward converter circuit diagram.

To illustrate the behavior of the forward converter with active-clamp reset, Fig. 2 shows the simulation results of the circuit in Fig. 1 with output-voltage feedback control during large-signal transients. Fig. 2(a) shows clamp-capacitor voltage V_C, magnetizing current of the transformer I_M, and output voltage of the error amplifier V_E during an input-voltage transient from 100 V to 200 V. Fig. 2(b) shows the same waveforms during a load transient from 18 A to 20 A. The circuit parameters used in the simulations using SIMPLIS simulation software [7] are: L_M=2.5 mH, C_C=22 nF, maximum duty cycle D_{max}=0.7, switching frequency f_s=100 kHz, and control loop crossover frequency f_c=3.6 kHz.

As can be seen from Fig. 2(a) and (b), the peak voltage of the clamp voltage and magnetizing current during transients are much larger than the ripple voltage and current in steady state. Therefore, for a proper design of the circuit, it is very important to understand the circuit performance and predict the maximum stresses of the components during large-signal transients.

Specifically, before the input-voltage transient, the converter in Fig. 2(a) operates with a large duty cycle and with a balanced flux in the core so that $V_{IN}\cdot D=V_C\cdot(1-D)$. Since after the line change, the duty cycle and the clamp-capacitor voltage V_C does not change instantaneously, the volt-second product becomes unbalanced, i.e., $V_{IN}\cdot D>V_C\cdot(1-D)$. As a result, the magnetizing current of the transformer starts increasing after the input-voltage change. The increased magnetizing energy charges the clamp capacitor, increasing the clamp-capacitor voltage. This transition continues until V_C becomes large enough so that the volt-second product becomes $V_{IN}\cdot D<V_C\cdot(1-D)$, and

0-7803-4489-8/98/$10.00 © 1998 IEEE

the magnetizing current of the transformer starts to decrease. The described clamp-capacitor voltage increase and the subsequent decrease after the transient can be seen as an oscillatory response of the resonant circuit consisting of the clamp capacitor and the magnetizing inductance of the transformer. Similar resonant behavior during load transient can be observed in Fig. 2(b).

If the forward converter circuit with the active-clamp reset is not correctly designed, the peak clamp-capacitor voltage and magnetizing current during input-voltage and load transients may cause an excessive voltage stress on the primary switch and/or saturation of the core of the transformer. Yet another problem that may happen during transients is that the body diode of auxiliary switch S_2 may conduct due to a positive magnetizing current at the instant when main switch S_1 is turned on, as indicated in Fig. 2(a). If the auxiliary-switch body diode is conducting when the main switch S_1 is turned on, a slow reverse-recovery of the body diode may cause the failure of the circuit because of the low-impedance current path through the clamp capacitor, the auxiliary-switch body diode, and the main switch [2].

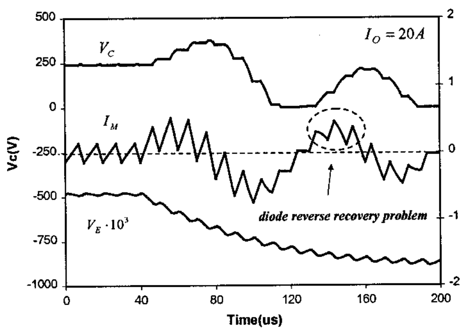

(a)

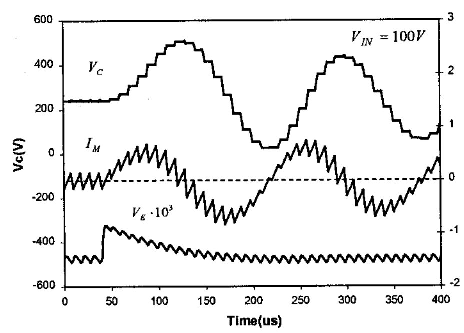

(b)

Fig. 2. Simulation results of large-signal transients of the forward converter with the active-clamp reset and output-voltage feedback control: (a) input-voltage step change from 100 V to 200 V; (b) load step change from 18 A to 20 A.

One approach to eliminate this problem is to connect a Schottky diode in series with the auxiliary switch to block the conduction of the body diode, and then to connect a fast-recovery anti-parallel diode around the series connection of the Schottky and the auxiliary switch [2]. The other approach is to design an active-clamp circuit, so that the magnetizing current is always negative at the instant main switch S_1 is turned on.

III. STATE TRAJECTORY OF ACTIVE-CLAMP RESET CIRCUIT

Fig. 3(a) and Fig. 3(b) are the simplified circuit diagrams during main switch S_1 turn-on and turn-off period, respectively. The state equations of v_c and i_m during S_1 on the period, Fig. 3(a), are

$$C_C \cdot \frac{dv_c}{dt} = 0 , \tag{1}$$

$$L_M \cdot \frac{di_m}{dt} = V_{in} . \tag{2}$$

By solving (1) and (2), the state trajectory during the on time of S_1 can be described as

$$v_c(t) = v_c(t_0), \tag{3}$$

$$i_m(t) = \frac{V_{in}}{L_M} \cdot t + i_m(t_0), \tag{4}$$

where $v_c(t_0)$ is the initial value of the clamp-capacitor voltage and $i_m(t_0)$ is the initial value of the magnetizing current of the transformer at the main-switch-on instant. The state trajectory during this period is a line parallel to i_m axis with a constant v_c, as shown in Fig. 4.

During the off period, Fig. 3(b), the state equations of v_c and i_m are

$$C_C \cdot \frac{dv_c}{dt} = i_m , \tag{5}$$

$$L_M \cdot \frac{di_m}{dt} = -v_c . \tag{6}$$

By solving (5) and (6), the state trajectory during the off time of S_1 can be described as

$$v_c(t) = r \cdot \cos[\alpha - \omega_o(t) \cdot t], \tag{7}$$

$$i_m(t) \cdot Z_O = r \cdot \sin[\alpha - \omega_o(t) \cdot t], \tag{8}$$

$$v_c(t)^2 + [i_m(t) \cdot Z_o]^2 = r^2 , \tag{9}$$

where,

$$r = \sqrt{v_c(t_1)^2 + i_m(t_1)^2 \cdot Z_o^{\ 2}} , \tag{10}$$

$$\alpha = \tan^{-1}\left(\frac{i_m(t_1) \cdot Z_o}{v_c(t_1)}\right), \tag{11}$$

$$\omega_o = \frac{1}{\sqrt{L_M \cdot C_C}} , \tag{12}$$

$$Z_o = \sqrt{\frac{L_M}{C_C}} , \tag{13}$$

$v_c(t_1)$ is the initial value of the clamp-capacitor voltage, and $i_m(t_1)$ is the initial value of the magnetizing current of the transformer at the turn-off instant of main switch S_1. The state trajectory during this period is shown in Fig. 4.

The solid line in Fig. 5 shows the state trajectory of the active-clamp reset circuit during the same input-voltage transient as in Fig. 2(a). The state trajectory starts with a closed cycle as described in Fig. 4. The dashed line in Fig. 5 shows the average-model state trajectory which has a simpler waveform than the state trajectory. The average state trajectory is going to be discussed later.

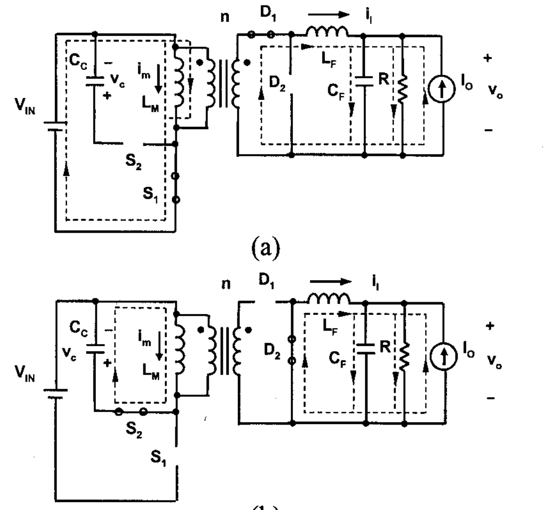

Fig. 3 Simplified circuit diagrams: (a) during the on period of main switch; (b) during the off period of main switch.

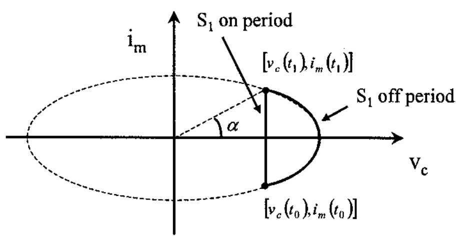

Fig. 4. The state trajectory of the active-clamp reset circuit in steady state.

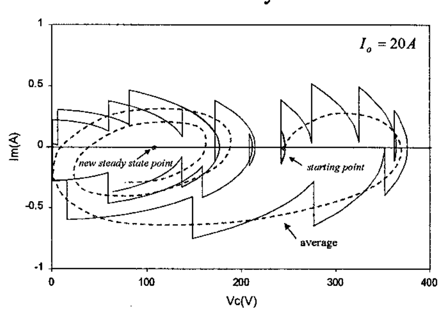

Fig. 5 The state trajectory of the active-clamp reset circuit during input-voltage step from 100 V to 200 V transient.

IV. DUTY CYCLE EQUATIONS DURING STEP INPUT-VOLTAGE AND LOAD TRANSIENTS

The transient behavior of the active-clamp reset circuit depends on the speed of the control and the characteristics of the resonant circuit. As can be seen from Fig. 2(a) and Fig. 2(b), the clamp voltage and magnetizing current transient waveforms show a resonant behavior with superimposed high switching-frequency ripples. Usually the resonant frequency is at least one magnitude smaller than the switching frequency in order to obtain a small ripple voltage of the clamp capacitor in steady state. Therefore, to simplify the analysis, the switching frequency ripples are ignored in the following analysis. However, the clamp voltage and magnetizing current ripples can be easily added into the results obtained by the simplified model later. As an illustration, Fig. 5 shows the relationship between state trajectory (solid line) and average state trajectory (dashed line).

A. Average model of the active-clamp forward converter

From Fig. 3(a) and Fig. 3(b), by ignoring the high switching frequency ripples, the average model of the active-clamp forward converter can be written as

$$C_F \cdot \frac{dv_o}{dt} = i_l + I_o - \frac{v_o}{R}, \tag{14}$$

$$L_F \cdot \frac{di_l}{dt} = \frac{d \cdot V_{in}}{n} - v_o, \tag{15}$$

$$L_M \cdot \frac{di_m}{dt} = d \cdot V_{in} - d' v_c, \tag{16}$$

$$C_C \cdot \frac{dv_c}{dt} = d' \cdot i_m, \tag{17}$$

where d is the duty cycle of main switch and d'=1-d.

Equations (16) and (17) can be rewritten as

$$\left(\frac{L_m}{d'}\right) \cdot \frac{di_m}{dt} = \frac{d}{d'} \cdot V_{in} - v_c, \tag{18}$$

$$\left(\frac{C_c}{d'}\right) \cdot \frac{dv_c}{dt} = i_m. \tag{19}$$

According to Eqs.(14)-(19), the average model of the forward converter power stage and the active-clamp reset circuit can be drawn as in Fig. 6(a) and Fig. 6(b), respectively. As can be seen from Fig. 6, the forward converter power stage and the active-clamp reset circuit are only coupled through the duty cycle. For the step input-voltage and load changes, the forward converter power stage represents a linear system. However, the average active-clamp reset circuit is nonlinear with respect to the duty cycle.

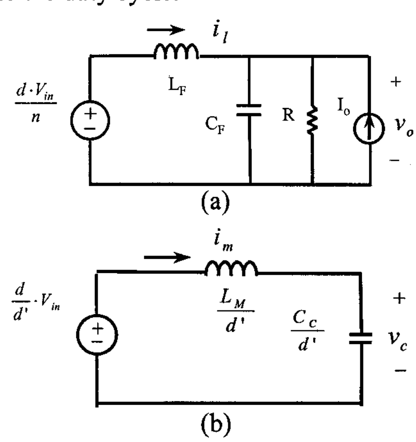

Fig. 6 The average model of the active-clamp forward converter: (a) average model of the forward converter power stage; (b) average model of the active-clamp reset circuit.

B. Duty cycle equations during line and load changes

To further study the transient behavior of the active-clamp circuit, it is necessary to know the duty cycle dependence during input-voltage and load changes. Assuming that the input-voltage perturbation is limited to a step change, and

$$\begin{aligned} V_{in\_new} &= V_{in\_old} + \Delta v_{in} \\ I_{o\_new} &= I_{o\_old} + \Delta i_o \\ D_{new} &= D_{old} + \Delta d \\ V_{o\_new} &= V_{o\_old} + \Delta v_o \end{aligned}, \qquad (20)$$

where Δv_{in} and Δi_o are the perturbations and Δd and Δv_o are the corresponding changes.

The perturbations of (1) and (2) yield

$$\Delta v_o = G_d \cdot \Delta d + G_v \cdot \Delta v_{in} + Z_o \cdot \Delta i_o , \qquad (21)$$

where,

$$G_v = \frac{\Delta v_o}{\Delta v_{in}} = \frac{\frac{D_{old}}{n}}{1 + s \cdot \frac{L_F}{R} + s^2 \cdot L_F \cdot C_F}, \qquad (22)$$

$$Z_o = \frac{\Delta v_o}{\Delta i_o} = \frac{s \cdot L_F}{1 + s \cdot \frac{L_F}{R} + s^2 \cdot L_F \cdot C_F}, \qquad (23)$$

$$G_d = \frac{\Delta v_o}{\Delta d} = \frac{\frac{V_{in\_new}}{n}}{1 + s \cdot \frac{L_F}{R} + s^2 \cdot L_F \cdot C_F}. \qquad (24)$$

Assuming the transfer function of control loop compensator is A(s), the loop gain is $T(s) = A(s) \cdot G_d(s)$ as shown in the closed-loop block diagram of the forward converter in Fig. 7. According to Fig. 7, the closed loop equations are

$$\frac{\Delta d}{\Delta v_{in}}\Big|close = \frac{\Delta d}{\Delta v_o} \cdot \frac{\Delta v_o}{\Delta v_{in}} = -\frac{D_{old}}{V_{in\_new}} \cdot \frac{T(s)}{1+T(s)}, \qquad (25)$$

$$\frac{\Delta d}{\Delta i_o}\Big|close = \frac{\Delta d}{\Delta v_o} \cdot \frac{\Delta v_o}{\Delta i_o} = -\frac{s \cdot L_F \cdot n}{V_{in\_new}} \cdot \frac{T(s)}{1+T(s)}, \qquad (26)$$

where, D_{old} is the duty cycle before perturbation, and V_{in_new} is the input voltage after the line step change.

Generally, neglecting the ESR zero of output-filter capacitor C_F, the optimal compensation of the output-voltage feedback control loop requires the transfer function of the compensator in the form

$$A(s) = \frac{A_{dc}}{s} \cdot \frac{(1 + s/\omega_{z1}) \cdot (1 + s/\omega_{z2})}{(1 + s/\omega_p)}, \qquad (27)$$

where, compensator zeroes ω_{z1} and ω_{z2} are placed to cancel two poles in G_d transfer function, i.e., ω_{z1} and ω_{z2} are close to $\frac{1}{\sqrt{L_F \cdot C_F}}$, and ω_p is placed at a frequency between crossover frequency ω_c and switching frequency ω_s [8].

Since when T>>1, $\frac{T}{1+T} \approx 1$, and when T<<1, $\frac{T}{1+T} \approx T$. The $\frac{T}{1+T}$ transfer function becomes

$$\frac{T}{1+T} = \frac{1}{(1 + s/\omega_c) \cdot (1 + s/\omega_p)}, \qquad (28)$$

as shown in Fig. 8.

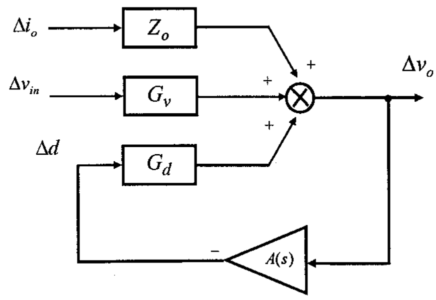

Fig. 7 Forward converter closed loop block diagram.

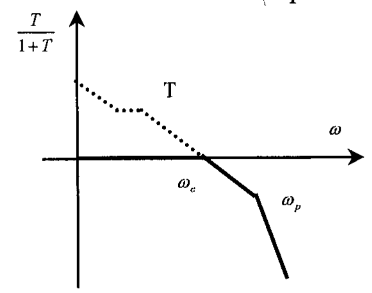

Fig. 8 T/(1+T) Bode plot.

Substituting (28) into (25) and (26), the closed-loop transfer functions are

$$\frac{\Delta d}{\Delta v_{in}}\Big|_{close} = -\frac{D_{old}}{V_{in\_new}} \cdot \frac{1}{(1 + s/\omega_c) \cdot (1 + s/\omega_p)}, \qquad (29)$$

$$\frac{\Delta d}{\Delta i_o}\Big|_{close} = -\frac{s \cdot L_F \cdot n}{V_{in\_new}} \cdot \frac{1}{(1 + s/\omega_c) \cdot (1 + s/\omega_p)}. \qquad (30)$$

Therefore, from (29), for a step input voltage change, the time domain equation for the duty cycle can be written as

$$d(t) = D_{old} + (D_{new} - D_{old}) \cdot \left(1 - \frac{\omega_p}{\omega_p - \omega_c} e^{-\omega_c \cdot t} + \frac{\omega_c}{\omega_p - \omega_c} e^{-\omega_p \cdot t} \right) \qquad (31)$$

Because generally ω_p is selected so that $\omega_p >> \omega_c$, (31) can be simplified to

$$d(t) = D_{old} + (D_{new} - D_{old}) \cdot \left(1 - e^{-\omega_c \cdot t}\right). \qquad (32)$$

Similarly, from Eq. (30), under the same assumptions, the time domain equation for the duty cycle during a step load change can be obtained as

$$d(t) = D_{old} - \frac{n \cdot \omega_c \cdot L_F}{V_{in}} \cdot \Delta I_o \cdot e^{-\omega_c \cdot t}. \qquad (33)$$

V. LARGE-SIGNAL TRANSIENT ANALYSIS

A. Average state trajectory equations

From Fig. 6, it can be seen that the average model of the active-clamp reset circuit is a nonlinear system whose parameters are the functions of the duty cycle. At the same time, the duty cycle is independent of the parameters of the L_M-C_C resonant network, i.e., it is decoupled from the state variables, v_c and i_m. In addition, since the duty cycle does not change during each switching period, the average model in Fig. 6(b) can be considered linear during each switching period with input voltage fixed at $\frac{d}{d'}\cdot V_{in}$, magnetizing inductance $\frac{L_M}{d'}$, and clamp capacitance $\frac{C_C}{d'}$.

By solving (18) and (19), the state trajectory equations during each switching period are

$$v_c(t)=r(0)\cdot\cos[\alpha(0)-\omega_o\cdot t]+v_{center}, \qquad (34)$$

$$i_m(t)\cdot Z_O=r(0)\cdot\sin[\alpha(0)-\omega_o\cdot t], \qquad (35)$$

where,

$$v_{center}=\frac{d}{d'}\cdot Vin, \qquad (36)$$

$$r(0)=\sqrt{[v_c(0)-v_{center}(0)]^2+i_m(0)^2\cdot Z_O{}^2}, \qquad (37)$$

$$\alpha(0)=\tan^{-1}\left(\frac{i_m(0)\cdot Z_O}{v_c(0)-v_{center}}\right). \qquad (38)$$

In (34) - (38), $v_C(0)$ is the initial average voltage of the clamp capacitor and $i_m(0)$ is the initial average magnetizing current of the transformer at the main switch on instant. $\omega_o=\frac{d'}{\sqrt{L_M\cdot C_C}}$ is the resonant frequency of L_M-C_C resonant network, and $Z_O=\sqrt{\frac{L_M}{C_C}}$ is the characteristic impedance of the resonant network.

By combining (34) and (35), the state trajectory equation can be written as

$$[v_c(t)-v_{center}]^2+[i_m(t)\cdot Z_O]^2=r(0)^2 \qquad (39)$$

It is an eclipse with center (v_{center}, 0) in the v_c-i_m state plane, and a circle in the $v_c-i_m\cdot Z_O$ state plane. The dynamic equilibrium point, v_{center}, is the center of the state trajectory and is a function of the duty cycle and the input voltage. The average state trajectory is shown in Fig. 9 with the solid line.

Because the duty cycle is a slow varying compared with a switching period, the duty cycle d(t) changes gradually during transient. Consequently, it can be assumed that the average state trajectory movement is a continuous movement with moving center $v_{center}(t)$ described by equations (34)-(39), where all quantities dependent on duty cycle are functions of time.

Similarly, one can analyze the average state trajectory in the presence of resistive loss R_M which represents a sum of the switch on resistance and the core loss of the transformer. The normalized average state trajectory with damping is shown in Fig. 9 with a dashed line. v_{center} is the spiral point of the state trajectory and the damping of the trajectory is $e^{-\frac{R_M}{2\cdot L_M}\cdot t}$.

Since time constant in the damping term is usually very large when no external damping circuit is used, the effect of the damping does not have a significant impact on peak values of state variables in the transient analysis. The rest of the paper will analyze the circuit's transient behavior without a damping effect.

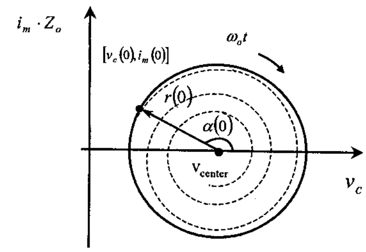

Fig. 9. Average state trajectory without damping (solid line); with damping (dashed line).

B. Movement of the average state trajectory during input-voltage transient

Before the input-voltage step change from V_{in_old} to V_{in_new}, the average state trajectory is a single point in the $v_c-i_m\cdot Z_o$ state plane with duty cycle d=D_{old}, initial average clamp-capacitor voltage $v_c(0)=\frac{D_{old}}{D_{old}'}\cdot V_{in\_old}$, and the average magnetizing current of the transformer $i_m(0)=0$. Since immediately after an input-voltage step change, the duty cycle cannot change instantaneously, the trajectory center after the change is $v_{center}(0)=\frac{D_{old}}{D_{old}'}\cdot V_{in\_new}$ and the average state trajectory follows the circle described in (39) with the center [$v_{center}(0)$, 0] and radius $r(0)=|v_{center}(0)-v_c(0)|$.

When the converter operates with the control loop open, i.e., has a fixed duty cycle, d does not change. Consequently, v_{center} and r do not change, and the state trajectory is a fixed circle as shown in Fig. 10. However, when the forward converter has an output-voltage feedback control, the duty cycle changes gradually from D_{old} to D_{new} as described in (32) so the center of the circle moves from $v_{center}(0)$ to $v_{c\_new}=\frac{D_{new}}{D_{new}'}\cdot V_{in\_new}$, which is the new steady state value of the clamp-capacitor voltage. The trajectory movement is illustrated in Fig. 11.

Fig. 11(a) and Fig. 11(b) are the state trajectories during input-voltage from 200 V to 300 V transient with a bandwidth f_c=3 kHz and f_c=20 kHz, respectively. Both state trajectories follow the open loop circle (dashed line) at the beginning of the transient. Since v_{center} moves faster in Fig. 11(b) due to a higher bandwidth, the state trajectory in Fig. 11(b) takes less time to move to the new steady state, and it results in a lower peak voltage of the switch and a lower peak magnetizing current (smaller thick solid-line circle).

Fig. 11(c) and Fig. 11(d) are the state trajectories during input-voltage from 300 V to 200 V transient with a bandwidth f_c=3 kHz and f_c=20 kHz, respectively. Similar state trajectory movements can be observed. As can be seen from Fig. 11, the worst case (largest thick solid-line circle) happens when the input-voltage steps from low to high, and the bandwidth is lowest.

The resonant frequency of the active-clamp circuit plays an important role, since the state trajectory is determined by two movements, the state trajectory center movement, whose speed is controlled by the bandwidth f_c; and the resonant movement, whose speed is determined by the resonant frequency f_o. Fig. 12 shows the calculated maximum values of v_c and i_m as functions of f_o/f_c. For the same bandwidth, a lower resonant frequency has a smaller peak clamp-capacitor voltage and peak magnetizing current.

The peak voltage of the main switch and the magnetizing current of the transformer can be calculated by adding the ripple as

$$i_m(peak)=i_{m\_ave}(\max)+\frac{1}{2}\cdot\frac{V_{in}\cdot D\cdot T_s}{L_M} \qquad (40)$$

$$v_{s1}(peak)=V_{in\_new}+v_{c\_ave}(\max)+\frac{1}{2}\cdot\frac{1}{8}\cdot\frac{D'\cdot n\cdot V_o\cdot T_s^2}{L_M\cdot C_C} \qquad (41)$$

C. Movement of state trajectory during load transient

Before a load step change, the average state trajectory is a single point in the $v_c - i_m\cdot Z_o$ state plane with duty cycle $d=D_{old}$, initial average clamp-capacitor voltage $v_c(0)=\frac{D_{old}}{D_{old}'}\cdot V_{in}$ and the average magnetizing current of the transformer $i_m(0)=0$. According to (33), at the moment of a step load change, the duty cycle changes for

$$\Delta d=-\frac{n\cdot\omega_c\cdot L_F}{V_{in}}\cdot\Delta I_o, \qquad (42)$$

so that the initial trajectory center is

$$v_{center}(0)=\frac{D_{old}+\Delta d}{D_{old}'-\Delta d}\cdot V_{in}. \qquad (43)$$

The average state trajectory follows the circle described in (39) with circle center at [$v_{center}(0)$, 0] and radius $r(0)=|v_{center}(0)-v_c(0)|$.

Because of the output-voltage feedback control, the duty cycle returns gradually to D_{old} as described in (33). Therefore, the center of the circle moves from $v_{center}(0)$ to $v_c(0)$, which is the original steady state value of the clamp-capacitor voltage, as illustrated in Fig. 13.

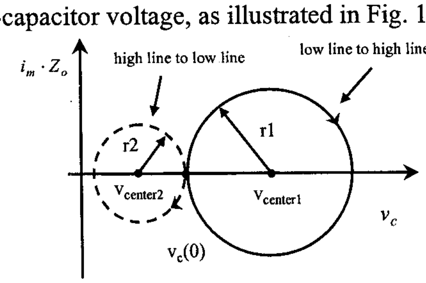

Fig. 10. Open-loop state trajectories during input step changes.

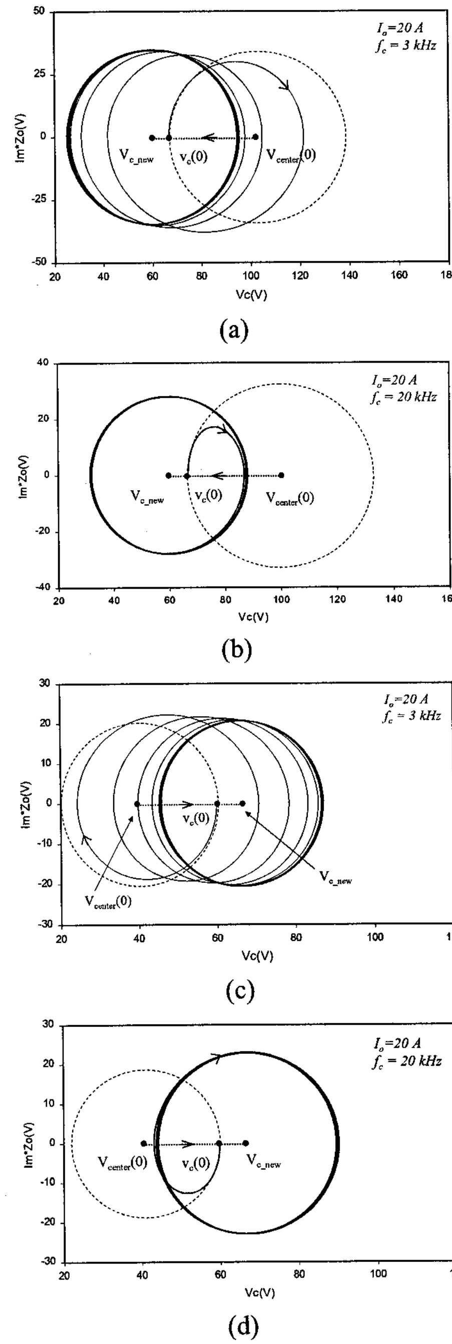

Fig. 11. Closed-loop average state trajectories with different bandwidths and input step changes: (a)-(b) input-voltage step from 200 V to 300 V; (c)-(d) input-voltage step from 300 V to 200 V.

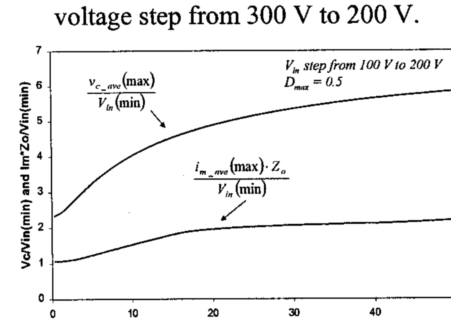

Fig. 12 The maximum average values of v_c and i_m are functions of f_o/f_c.

Fig. 13(a) and Fig. 13(b) are the state trajectories during a step load change from 18 A to 20 A with a bandwidth of f_c=3 kHz and f_c=20 kHz, respectively. Both state trajectories follow the open loop circle (dashed line) at the beginning of the transient. Since v_{center} moves faster in Fig. 13(b) due to a higher bandwidth, the state trajectory in Fig. 13(b) takes less time to move to the new steady state. It should be noted that according to (33), the circuit with higher control bandwidth has a larger initial duty cycle jump. As a result, the initial radius r(0) is much larger for the high bandwidth case. This is opposite to the case of a step input-voltage change, where the circuit with a higher bandwidth control experiences a larger maximum clamp-capacitor voltage and magnetizing current.

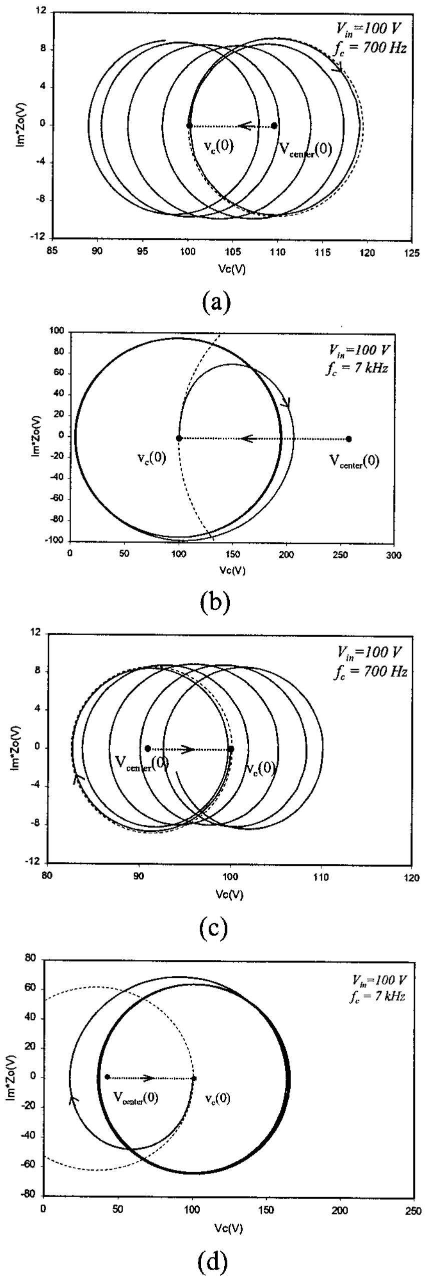

Fig. 13. Closed-loop average state trajectories with different control bandwidths and load step changes: (a)-(b) load current step from 18 A to 20 A; (c)-(d) load current step from 20 A to 18 A.

Fig. 13(c) and Fig. 13(d) show the state trajectories during a step load change from 20 A to 18 A with a bandwidth f_c=3 kHz and f_c=20 kHz, respectively. As can be seen from Fig. 13, the maximum transient voltage stress of the switch and the maximum transient magnetizing current occur for a positive step load change with a high bandwidth. For the same bandwidth, a lower resonant frequency has a smaller peak clamp-capacitor voltage and peak magnetizing current.

In addition, the minimum input-voltage condition exhibits the largest clamp-capacitor voltage and the magnetizing current transient since $v_{center}(0)$ is the largest due to the smallest d'. A smaller output-filter inductance helps to reduce the duty cycle change during transients and reduces the peak voltage and the magnetizing current.

VI. SUMMARY

The large-signal transient analysis of the forward converter with the active-clamp reset and the output-voltage feedback control is presented in this paper. Based on the analysis, the circuit performance during large-signal line and load transients can be predicted. It is shown that the ratio of the control bandwidth to resonant frequency is a design parameter of the maximum clamp-capacitor voltage and magnetizing current values. By using this analytical approach, the circuit design issues, such as the switch voltage stress, transformer saturation, and reverse recovery problems in the anti-parallel diode of the active-clamp switch can be addressed.

REFERENCES

[1] P. Vinciarelli, "Optimal resetting of the transformer's core in single ended forward converters," U.S. Patent, No. 4,441,146, Apr. 1984.

[2] B. Carsten, "Design techniques for transformer active reset circuits at high frequencies and power levels," High Frequency Power Conversion Conf. Proc., pp. 235-246, 1990.

[3] B. Andreycak, "Active clamp and reset technique enhances forward converter performance," Unitrode Power Supply Design Seminar, SEM-1000, pp. 3-1 - 3-18, 1994.

[4] D. Dalal and L. Wofford, "Novel control IC for single-ended active clamp converters," High Frequency Power Conversion Conf. Proc., pp. 136-146, 1995.

[5] C. S. Leu, G. Hua, and F. C. Lee, "Comparison of forward topologies with various reset schemes," High Frequency Power Conversion Conf. Proc. pp. 198-208, 1992.

[6] I. D. Jitaru, "Constant frequency, forward converter with resonant transition," High Frequency Power Conversion Conf. Proc., pp. 282-292, 1991.

[7] SIMPLIS user's manual, Power Design Tools Inc., Release 2.5, September 1994.

[8] F. C. Lee, Z. D. Fang, and T. H. Lee, "Optimal design strategy of switching converters employing current injected control," IEEE Trans. on Aerospace and Electronic Systems, Vol. AES-21, No.7, pp. 21-35, January 1985.